Arctic, Antarctic, and Alpine Research, Vol. 44, No. 2, 2012, pp. 210–221

Loss of Multiyear Landfast Sea Ice from Yelverton Bay, Ellesmere Island, Nunavut, Canada

*Sierra Pope**
Luke Copland‡ and*
Derek Mueller†

*Department of Geography, University of Ottawa, Ottawa, Ontario K1N 6N5, Canada
†Department of Geography and Environmental Studies, Carleton University, Ottawa, Ontario K1S 5B6, Canada
‡Corresponding author: luke.copland@uottawa.ca

Abstract

For much of the 20th century, multiyear landfast sea ice (MLSI) formed a permanent ice cover in Yelverton Bay, Ellesmere Island. This MLSI formed following the removal of ice shelf ice from Yelverton Bay in the early 1900s, including the well-documented Ice Island T-3. The MLSI cover survived intact for 55–60 years until 2005, when >690 km^2 (90%) of MLSI was lost from Yelverton Bay. Further losses occurred in 2008, and the last of the Yelverton Bay MLSI was lost in August 2010. Ground penetrating radar (GPR) transects and ice cores taken in June 2009 provide the first detailed assessment of MLSI in Yelverton Inlet, and indeed the last assessment now that it has all been replaced with first-year ice. A detailed history of ice shelf, glacier, and MLSI changes in Yelverton Bay since the early 1900s is presented using remotely sensed imagery (air photos, space-borne optical, and radar scenes) and ancillary evidence from *in situ* surveys. Recent changes in the floating ice cover here align with the broad-scale trend of long-term reductions in age and thickness of sea ice in the Arctic Ocean and Canadian Arctic Archipelago.

DOI: http://dx.doi.org/10.1657/1938-4246-44.2.210

Introduction

Sea ice in the Arctic Ocean has undergone dramatic recent changes. The rate of change in Arctic sea ice extent at the end of the melt season from 1953 to 2006 was −7.8% per decade (Stroeve et al., 2007), and this rate is even higher (−12.4% per decade) over the period of satellite measurements (1979–2010) (Stroeve et al., 2011). Sea ice area decreases have been most pronounced during the month of September (Serreze et al., 2007); the last five years (2007 to 2011) have featured the five lowest September ice extents in the satellite record (NSIDC, 2011). In addition to the negative trends in northern hemisphere summer minimum extent along with winter area, several recent studies have determined reductions in age and thickness of multiyear ice in the Arctic Ocean (Rothrock et al., 1999; Maslanik et al., 2007, 2011), particularly in the eastern Arctic Ocean (Rigor and Wallace, 2004; Nghiem et al., 2006). Kwok and Rothrock (2009) reported a decrease in mean sea ice thickness over the Arctic Ocean from 3.64 m in 1980 to 1.89 m in 2008. As thick, perennial sea ice is more likely to survive the summer melt season, a smaller proportion of perennial ice will negatively impact future sea ice extents in the Arctic Ocean (Maslanik et al., 2007; Nghiem et al., 2007).

The presence and behavior of this multiyear sea ice (MYI) has been studied in detail in the Canadian Arctic Archipelago (CAA), the group of islands north of mainland Canada. The regional average September MYI area changed at a rate of −4.1% per decade from 1968 to 2008 (Tivy et al., 2011) and −6.4% per decade from 1979 to 2008 (Howell et al., 2009). However, these decreases are not statistically significant, with Tivy et al. (2011) and Howell et al. (2009) explaining that reductions of *in situ* MYI formation in the CAA have been largely balanced by increased import of MYI from the Arctic Ocean. Adding to the complexity of the region's MYI measurements, much of the CAA features sea ice which remains predominantly landfast for 6–8 months of the year (Melling, 2002), and the movement of sea ice between the Arctic Ocean and the CAA is impacted by the presence of landfast ice blockages (Alt et al., 2006; Howell et al., 2009; Kwok, 2006).

The protective nature of the many channels in the CAA, and the tendency of the Beaufort Gyre to force thick multiyear ice against the NW edge of the CAA, has led to the formation of several semi-permanent multiyear landfast sea ice (MLSI) features there. MLSI has historically formed plugs in Sverdrup Channel and Nansen Sound in the northern CAA (Jeffers et al., 2001) and has developed around the ice shelves found on the NW coast of Ellesmere Island (Jeffries, 1987). The stability of ice shelves is associated with the presence of a stable MLSI fringe (Copland et al., 2007; Reeh et al., 2001), with dramatic losses of ice shelves along northern Ellesmere Island in the last decade frequently occurring during periods of extended open water after periods of significant MLSI loss (Copland et al., 2007; Mueller et al., 2008).

This study combines fieldwork and remote sensing image analysis to provide the first quantification of the characteristics and changes in MLSI over the last 60 years in Yelverton Bay and Yelverton Inlet, Ellesmere Island (Fig. 1). Ice cores were extracted in Yelverton Inlet in June 2009 to provide detailed identification of sea ice types and characteristics. These cores were used to verify ground-penetrating radar (GPR) measurements in Yelverton Inlet, which establish sea ice thickness, sea ice internal structure, and snow depths. This information is then used to identify ice types on RADARSAT-2 and Advanced Spaceborne Thermal Emission and Reflection Radiometer (ASTER) images from the same year. These results provide improved understanding of the ability of synthetic aperture radar (SAR) to remotely determine ice types, and enable improved mapping of sea ice changes in the region since the early 1950s using air photos in addition to RADARSAT, MODIS (Moderate Resolution Imaging Spectroradiometer), and ASTER satellite scenes (Table 1).

1523-0430/6 $7.00

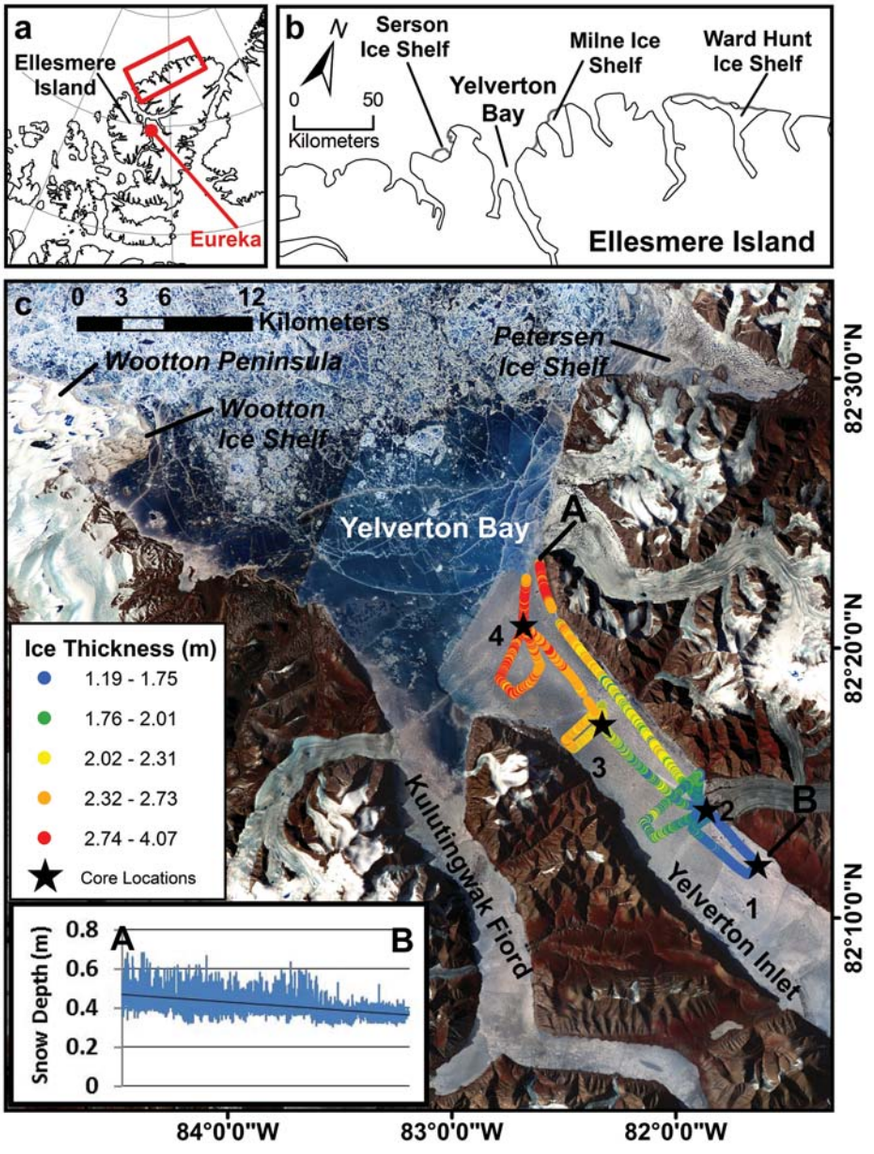

FIGURE 1. (a) Location of study site on northern Ellesmere Island. (b) NW coast of Ellesmere Island showing location of Yelverton Bay and ice shelves as of July 2009. (c) ASTER mosaic (July 2009, see Table 1 for acquisition dates) of Yelverton Bay and surrounding features, ice core locations, and ice thicknesses derived from GPR surveys on 2 June 2009. Inset graph shows GPR-derived snow depth profile from Point A to B.

Study Site

Yelverton Bay, on the NW coast of Ellesmere Island in the CAA, lies between the Serson and Milne Ice Shelves and extends across the front of the Petersen Ice Shelf (Fig. 1). Two fiords, Yelverton Inlet and the smaller Kulutingwak Fiord, extend southeast and south from the bay (Fig. 1, Part c). The terrain along the coast is mountainous and glaciated, and movement of glacier ice into the coast's fiords has historically resulted in thick ice shelves there (e.g., Milne Ice Shelf up to 100 m thick; Mortimer, 2011). Environment Canada Climate Normals (1971–2000) for Eureka Station (79°58.8′N, 85°55.8′W), ~330 km south of Yelverton Bay, indicate an average annual temperature of −20 °C and average annual precipitation of 75 mm. There are no long-term climate records available from the NW coast of Ellesmere Island, but recent short-term records for 2009–2010 indicate a mean annual temperature of −16.8 °C at nearby Milne Ice Shelf (http://tinyurl.com/milnewx).

In the early 1900s, a single ice shelf covering an estimated 8900 km^2 spanned nearly 500 km of the NW coast of Ellesmere Island (Vincent et al., 2001). This ice shelf fringe was thought to have formed between 3000 and 5500 years ago (England et al., 2008) from MLSI that gained mass via surface accumulation and basal accretion, along with contributions of glacier ice in places (Jeffries, 1987; Mueller et al., 2006). Over the 20th century this 'Ellesmere Ice Shelf' lost 90% of its extent and was reduced to six principal ice shelves (Mueller et al., 2006). Within the last decade, further ice shelf calving has occurred, with total losses of the Ayles Ice Shelf in 2005 (Copland et al., 2007) and the Markham Ice Shelf in 2008 (Mueller et al., 2008) creating new ice shelf–free fiords.

It is well documented that Yelverton Bay was occupied by an ice shelf at the beginning of the 20th century. Both Lt. Pelham Aldrich of the British Arctic Expedition and Cmdr. Robert Peary of the U.S. Navy described characteristic ''ice rollers'' while crossing Yelverton Bay in 1876 and 1906, respectively (Koenig et al., 1952).

TABLE 1

List of imagery used in the study.

Sensor/Data set	Resolution (m)	Acquisition Date (mm/dd/yyyy), Time (UTC, hh:mm), Image ID (where applicable)
ERS-1 Standard Beam[1]	30	05/19/1993, (00:27); 10/25/1994, (12:25)
RADARSAT ScanSAR Wide[1]	75 & 100	02/02/2000, (21:11); 08/05/2005, (20:15); 08/08/2005, (20:28); 08/18/2005, (20:36); 09/24/2005, (20:58); 04/27/2006, (19:45)
RADARSAT Standard Beam 1[1]	28	08/04/2004, (19:50); 03/18/2005, (19:58); 06/05/2005, (19:54); 07/16/2005, (19:58); 04/20/2006, (19:50)
RADARSAT Fine Beam 1[1]	10	02/14/2008, (21:33)
RADARSAT-2 Wide Beam[2]	40	03/05/2009, (20:17); 03/15/2009, (20:26); 03/03/2010, (13:50)
Aerial Photography (1950 Oblique, 1959–1984 Nadir)	≈0.8–3.0	08/1950, (Rolls T405R & T405L); 06/1959–08/1959, (Rolls A16606, A16688, A16706, A16724, A16728, A16734 & A16785); 07/11/1974, (Roll A23943); 07/23/1984, (Roll A26535)
MODIS TERRA	250	07/30/2008, (19:45); 08/30/2008, (18:50); 08/03/2008, (19:20); 08/05/2008, (22:25); 08/06/2008, (18:10); 08/07/2008, (22:10); 08/12/2008, (20:50); 08/14/2008, (20:40); 08/16/2008, (22:05); 08/19/2008, (17:40); 08/25/2008, (20:20); 08/31/2008, (19:45); 10/09/2008, (19:40), 08/22/2010, (22:05)
MODIS AQUA	250	08/02/2008, (14:05)
ASTER Level 1B	15	07/10/2009, (10:55); 07/13/2009, (23:26); 07/14/2009, (20:53); 07/16/2009, (20:41); 07/22/2009, (20:04)

[1] Frequency 5.3 GHz, Wavelength 5.656 cm, Polarization HH.
[2] Frequency 5.4 GHz, Wavelength 5.546 cm, Polarization HH.

In 1953, the bay was covered by MLSI (Hattersley-Smith, 1955), implying that Yelverton Bay was a significant source of ice islands, tabular icebergs calved from Arctic ice shelves, in the interim (Jeffries, 1987, 1992). Ice Island T-3 was the first to be identified as originating from Yelverton Bay (Jeffries, 1987). Seismic measurements across this ice island in 1952 indicated ice thicknesses ranging from 40 to 53 m (Crary, 1958), with its rolling topography and surficial rock material indicating an ice shelf source (Hattersley-Smith, 1957a, 1957b). Morainal material and plant remains found on Ice Island T-3 suggest that it originated from ice shelf ice deep within Yelverton Bay (Crary, 1960), and dendrochronological dating indicates that it calved between 1935 and 1947 (Polunin, 1955). However, it is likely that T-3 calved no later than the summer of 1946 since it was photographed 50 km north of Cape Isachsen on 27 April 1946 (Koenig et al., 1952). Jeffries (1987, 1992) suggested that Ice Islands T-1 and T-2 might also have originated in outer Yelverton Bay. The less distinct rolling texture observed on these ice islands is attributed to greater weathering and/or surface accumulation following their removal from the bay, as T-1 and T-2 calved prior to the removal of T-3 (Koenig et al., 1952). Area estimates of T-1, T-2, and T-3 suggest that over 1300 km^2 of ice shelf ice was lost (Koenig et al., 1952), emptying Yelverton Bay and leaving only a small area of ice shelf ice near Wootton Peninsula, at the NW corner of Yelverton Bay (Fig. 1).

Following this massive removal of ice shelf ice, sea ice formed and remained in place in the protected embayment. Over a period of decades in the latter half of the 20th century, this stable MLSI reached substantial thicknesses in Yelverton Bay, forming an incipient ice shelf (Hattersley-Smith, 1955). Meltponding and a dominant wind direction led to the formation of rolling surface features on this MLSI similar to those of ice shelves, albeit on a smaller scale (Jeffries and Sackinger, 1990a).

Methods

ICE CORE MEASUREMENTS

Field measurements were conducted in Yelverton Inlet, where shallow ice cores were drilled through the entire sea ice thickness (~1–3 m) with a Kovacs Mark II ice coring system with an internal diameter of 8.8 cm. Immediately after core extraction, ice temperatures were measured with probe thermometers inserted into holes drilled at 10 cm intervals into the center of the core. Visual observation of internal characteristics of the ice core were also made, including color, cloudiness, and the presence, size, and patterns of bubbles. Ice cores were then cut into 10-cm sections, which were photographed and melted within 24 hours for conductivity measurement using a temperature-corrected YSI probe. Temperature and salinity profiles along with the visible characteristics of the cores were compared with descriptions of sea ice types and FYI (first year ice)/MYI profiles in reference texts (Johnston and Timco, 2008; Wadhams, 2000). This allowed for age classification of the sampled sea ice. Ice thickness at the core sites was measured using a Kovacs Ice Thickness Gauge, lowered into the empty boreholes. Snow pits at each of the ice core locations were completed to measure snow depth, stratigraphy, and changes in crystal structure through the snowpack, as well as density at each of the snow layers.

GROUND PENETRATING RADAR MEASUREMENTS

A Pulse EKKO Pro 250 MHz Ground Penetrating Radar (GPR) system was used to collect ice thickness data in a reflection-type survey. The antennas were separated by 0.4 m, custom fitted into a sled, and towed behind a snowmobile at ~20 km hr^{-1}. Since there was a possibility of traveling over ice shelves, a total sampling depth of 300 ns was chosen to ensure that the entire ice thickness was measured. The GPR sampled at an interval of 0.4 ns. Simul-

taneous single frequency GPS measurements ($\sim \pm 5$ m horizontal accuracy) were taken at every GPR trace to enable mapping of the results. GPR measurements were conducted in transects throughout Yelverton Inlet, including the sites of ice core extraction.

To enhance the visibility of basal and internal reflector horizons (IRHs), post-processing of the GPR data was undertaken using EKKO_View software. The GPR lines were initially cut by position to exclude any data collected while the sled was not in motion. A Dewow filter was applied to reduce low frequency noise near the start of each trace, and trace differencing (a high-pass spatial filter) was completed to enhance rapidly changing profile features and suppress constant features in the GPR data. The Spherical Exponential Calibrated Compensation (SEC2) gain was used to compensate for spherical spreading losses and dissipation of the radar signal. Significant differences in the dielectric constants of snow, ice, and salt water, evident in the post-processed GPR traces, were used to isolate the snow-ice interface, the ice-water interface, and internal ice layering; the locations of these interfaces were confirmed with borehole measurements. Two-way travel time was then converted into snow and ice thickness values using the equation

$$T = ([(t + s/0.3)V_1/2]^2 - s^2/4)^{1/2} \quad (1)$$

where T is thickness (m), t is two-way travel time (ns), s is antenna separation (m), and V_1 is electromagnetic wave velocity (m ns^{-1}).

AERIAL PHOTOGRAPHY

A search was completed at the National Air Photo Library (NAPL), Ottawa, Canada, for air photos taken over Yelverton Bay and Yelverton Inlet. Air photos were scanned in grayscale at 600 dpi from NAPL prints and cropped to exclude framing. Royal Canadian Air Force (RCAF) Trimetrogon (T-Series) air photographs from August 1950 provide oblique, but not nadir, coverage of Yelverton Bay (Table 1). Varying look angles in the oblique T-Series air photographs made orthomosaicking impossible, but the images provide coverage of Yelverton Bay and Inlet, and were used for qualitative assessment of MLSI presence, as well as comparison with features in later images.

Stereo aerial photos taken by the RCAF between July and August 1959 provide almost complete coverage of Yelverton Bay, Yelverton Inlet, and nearby Kulutingwak Fiord, and were georeferenced to a 15-m resolution ASTER image from July 2009 (Fig. 1). Each photograph was georeferenced in ArcGIS 9.2 using a minimum of 20 ground control points, chosen preferentially over permanent land features widely spaced across the image to create as uniform and complete coverage as possible. A first order polynomial interpolation was used to georeference 94% of the photos; a third order polynomial was used for photos requiring a higher degree of warp to accommodate mountainous terrain. All vertical air photos were georeferenced with a root mean squared error (RMSE) of <15 m and mosaicked together in ENVI 4.3.

RCAF air photos from 1974 and 1984 were also collected (Table 1). These years provide very limited coverage of the Yelverton Bay area due to sparse and largely coastal flightlines, and limited snow-free ground cover made accurate georectification impossible. The images were catalogued to provide qualitative estimates of MLSI presence in Yelverton Bay, but were not relied upon for analysis.

SATELLITE IMAGERY

An extensive search was made to catalogue all available satellite imagery for the study area (Table 1). The SAR satellite scenes include ERS-1 imagery from 1993 and 1994, RADARSAT-1 imagery from 2000 to 2008, and RADARSAT-2 imagery from 2009 to 2010. These images allowed for the determination of MLSI, FYI, and ice shelf ice extent based on texture and tone differences. The classification of sea ice via SAR signature has been used in numerous studies (e.g., Askne and Dierking, 2008) and is used operationally by the Canadian Ice Service (CIS); guidelines for classification are outlined by Johnston and Timco (2008). Winter and early spring SAR scenes were used whenever possible, when the ice/snow surface was cold and dry. Ice types in Yelverton Inlet at the time of sampling were identified and delineated using a RADARSAT-2 image (acquired on 5 March 2009) using the methods described above. The image was then calibrated to extract the average normalized radar cross section (σ^0) from representative areas (totaling $\sim$30,000 pixels) in each ice type.

For a quantitative comparison of MLSI area changes with the 1959 air photo mosaic, 8 clear-sky, georectified ASTER L1B images from July 2009 were downloaded from NASA's Earth Observing System Data Gateway. The 15-m resolution ASTER scenes were co-registered and then mosaicked together in ENVI 4.3. Polygon differencing was used to quantify the change in MLSI area between 1959 and 2009. Areas of interest within the study region were highlighted to catalogue changing ice shelf, MLSI, and glacier extent, including the Wootton Peninsula Ice Shelf and Kulutingwak Fiord (Fig. 1). Finally, 250-m resolution MODIS imagery was collected over summers 2008 and 2010 to chart the removal of Yelverton Bay MLSI in periods when other higher resolution imagery was not available.

Results and Discussion

ICE CORE RESULTS

Shallow ice cores (Fig. 2, Part a) indicate variations in depth, salinity, and temperature of sea ice in Yelverton Inlet. Cores 1 and 2, taken at the back of the inlet, indicate ice thicknesses of 1.57 m and 1.41 m, respectively (Fig. 2, Part a). Salinities exhibited little variation in these cores, increasing with depth from <1 psu to ~ 2 psu. Temperature measurements ranged from -2.7 °C at the ice surface to -1.1 °C at the ice base. The salinities and uniformity of the profiles suggest that this sea ice formed over one winter, as a second or multiyear profile would indicate more than one ice type with a definite salinity demarcation (Johnston and Timco, 2008). The cores were cloudy in appearance, with small, linear bubbles present throughout, which may have been indicators of brine inclusions (Wadhams, 2000).

Cores 3 and 4 (Fig. 2, Part a) appeared distinctly different from the previous cores: they were 2.46 m and 2.54 m thick, respectively, with low salinities (<1 psu) from the surface to $\sim$1.70 m depth, increasing sharply to >5 psu from $\sim$1.70 m to the base. Temperatures of the cores remained stable between -6 and -4 °C from the surface down to $\sim$1.70 m, then rapidly increased to just above -2 °C at the base (Fig. 2, Part a). These temperature and salinity patterns of steady low values from the surface to approximately halfway down the core, then sharp salinity increases

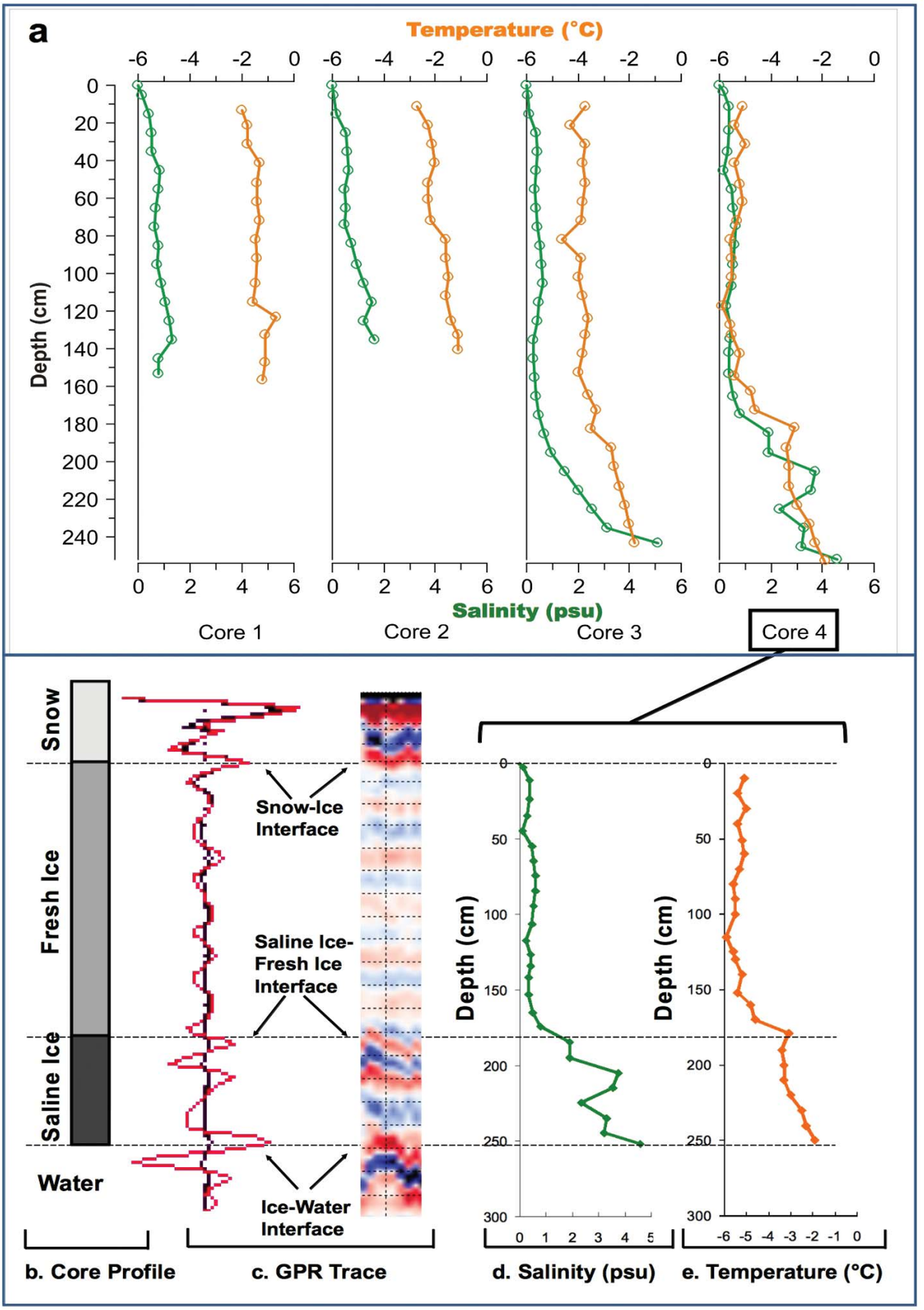

FIGURE 2. Ice core analysis in Yelverton Inlet. (a) Depth, temperature, and salinity measurements from ice cores 1–4 (locations in Fig. 1, Part c). Vertical ice stratigraphy at Core 4: (b) Ice type, (c) GPR record, wiggle trace (left) and color trace (right), (d) Salinity, (e) Temperature.

and temperature decreases, are a match to the profiles for multiyear sea ice outlined by Johnston and Timco (2008) and Wadhams (2000). The distinction between the upper and lower sections of Cores 3 and 4 were also evident in the visual observations. The cores featured frequent small bubble inclusions in a matrix of relatively clear ice from 0 m to between 1.75 and 1.86 m, then appeared cloudy to the base of the core. This is consistent with the theoretical growth of multiyear sea ice, with brine expulsion creating a nearly fresh layer of ice near the surface and concentrating brackish saltwater inclusions near the base of the core (Wadhams, 2000).

ICE THICKNESS DETERMINATION

Identification of signal reflections at the ice-water interface in the GPR transects was complicated by signal attenuation caused by density contrasts between the ice crystals and salty brine inclusions (Kovacs and Morey, 1978; Woodward and Burke, 2007). Of the 40,911 GPR traces recorded in Yelverton Inlet, only 25,388 showed clear ice base (i.e., ice-water) reflections. The two-way travel time of the radar and subsequent ice thickness value was established for each of these 25,388 points. To determine the correct radar velocity for calculating ice thicknesses (V_I), a value was chosen that provided the best fit to the *in situ* thicknesses recorded in the ice coring. A radar velocity of 0.150 m ns^{-1} provided the best fit using this process, with ice core thicknesses remaining within 1 standard deviation of the averaged GPR-derived thicknesses within 100 m of each core site. Similar velocities have been used in past sea ice studies: radar velocities of 0.156 and 0.157 m ns^{-1} were used on MYI measurements by Kovacs and Morey (1978) with a 625 MHz GPR system. A study of floating FYI in Mikkelsen Bay, Alaska, used radar velocities between 0.154 and 0.167 m ns^{-1} with a 200 MHz GPR system (Nyland, 2004). More recently, a controlled experiment with a 1000 MHz airborne GPR system used sea ice of known thickness (70 cm) to model a radar velocity of 0.140 m ns^{-1} (Bradford et al., 2010).

With a radar velocity of 0.150 m ns^{-1} and GPR sampling interval of 0.4 ns, the precision of the depth measurements (based on two-way travel time) is ~0.03 m. The GPR-derived sea ice thicknesses in Yelverton Inlet averaged 2.06 m with a standard deviation of 0.46 m, ranging from 1.19 m at the inland points to 3.71 m near the mouth of the inlet (Fig. 1, Part c). These thickness variations correspond with RADARSAT image signature differences and aided in the determination of ice types.

SNOW DEPTH DETERMINATION

The strong reflection in the GPR traces at the snow-ice interface allowed for determination of snow depths across the study area using a learned wavelet routine in Ice Picker R4 software. Using a radar velocity of 0.200 m ns^{-1}, as established by previous GPR snowpack studies (Annan, 2002), snow depths were determined over all GPR traces in Yelverton Inlet (Fig. 1). Average snow depth was 0.45 m, with a standard deviation of 0.08 m. Calculated snow depths along the GPR lines were verified by comparing the snow pit depth measurements at the core sites to the average values derived from GPR data collected within a 10-m radius of each pit. Snow depths at core sites 1, 2, and 3 were 0.37 m, 0.47 m, and 0.39 m, respectively, all well within 1 standard deviation of the average GPR-derived snow depth values of 0.35 m, 0.44 m, and 0.42 m. This suggests that a radar velocity of 0.200 m ns^{-1} is appropriate for the local snowpack. At Core 4, snow depth was measured at 0.71 m, whereas nearby GPR-derived depths averaged 0.44 m. A highly variable snowpack and surface rolls were observed around this site, so it is suspected that these local factors accounted for the particularly high snow depth at the core site.

Overall, GPR-derived snow depth measurements indicate that thicker snow is found at the mouth of Yelverton Inlet and into Yelverton Bay, with depths decreasing with distance southeastwards into the inlet (inset graph, Fig. 1, Part c). This trend of greater snow accumulation near the coast appears to be common along northern Ellesmere Island and driven by the primary Arctic Ocean moisture source in this region, although it has been poorly quantified before. The growth of MLSI and ice shelf ice relies in part on the accumulation of snow at the ice surface. Lower snow accumulation inland suggests that losses at the front of landfast ice features are not being balanced by new ice formation and/or glacier flow from inland, leaving the inland ice more vulnerable to melt and breakup. This could be a factor in the recent negative trends in ice shelf mass balance reported at Ward Hunt Ice Shelf (Braun et al., 2004) and Ayles Ice Shelf (Copland et al., 2007).

COMPARISON OF ICE CORE PROPERTIES WITH GPR TRACES

The differences in ice thickness and type found in the ice cores were also visible as differences between GPR traces collected in different parts of Yelverton Inlet (Fig. 3). Traces from Line 2, at the rear of the inlet (Fig. 3, Part a), show a single smooth reflector at the ice base (i.e., ice-water interface), visible as a peak in the GPR record. In comparison, GPR traces near the mouth of Yelverton Inlet show a weak and variable ice base reflection, but a new internal reflector horizon (IRH; Fig. 3, Part b). This IRH corresponds with the interface between fresh and saline ice found in Cores 3 and 4 (Fig. 2). The Core 4 profile (Fig. 2, Parts b to e) indicates that the IRH occurs when the ice reaches a salinity of ~2 psu, with a corresponding increase in ice temperature, decrease in air bubble inclusions, and increase in ice cloudiness.

SATELLITE IMAGE ANALYSIS

The 2009 ice thickness and ice core measurements were compared with visual interpretation of the July 2009 ASTER images, field observations, and the brightness and texture of the 5 March 2009 RADARSAT-2 image. The intensity of backscatter in SAR imagery is dependent on the proportion of microwave energy that is returned to the satellite after reflecting off the ice surface and scattering within an ice volume beneath the surface. This geophysical information indicates distinct surface and internal characteristics, which differ between ages and types of sea and glacier ice (Askne and Dierking, 2008; Johnston and Timco, 2008). This enabled the determination of three sea ice types in Yelverton Inlet on the 5 March 2009 RADARSAT-2 image, as delineated in Figure 4. The ice at the mouth of the inlet had the brightest tone (highest

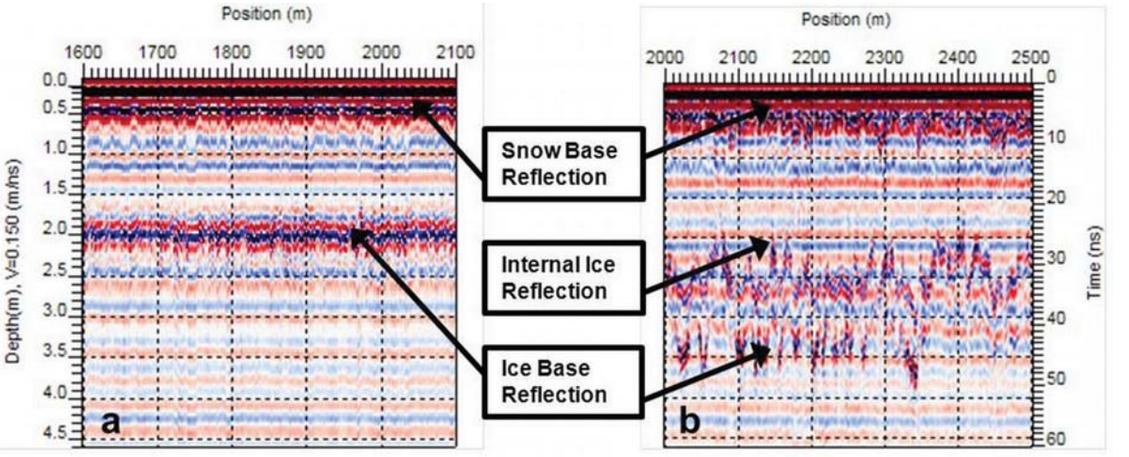

FIGURE 3. Traces of 500 m sections from two GPR lines in Yelverton Inlet (Fig. 1, part c). (a) Traces over FYI at rear of Yelverton Inlet near Core 1. (b) Traces over MLSI at the mouth of Yelverton Inlet near Core 4.

backscatter, $\sigma^0 = -10.9$ dB), likely due to low salinities and greater bubble concentration within the first meter below the surface (see Cores 3, 4 in Fig. 2, Part a). This allows for increased radar penetration and volume scattering within the ice, creating a strong return on the image and a brighter signature than would appear over FYI (Johnston and Timco, 2008). GPR-derived ice thicknesses over this region average 2.58 m (Fig. 1, Part c), and depths at Cores 3 and 4 are similarly thick (Fig. 2, Part a). As described above, the temperature and salinity profiles of these cores are considered to be representative of multiyear ice. Field observations of this ice identified distinctive surface rolls; MLSI is the only type of sea ice known to exhibit this type of rolling surface

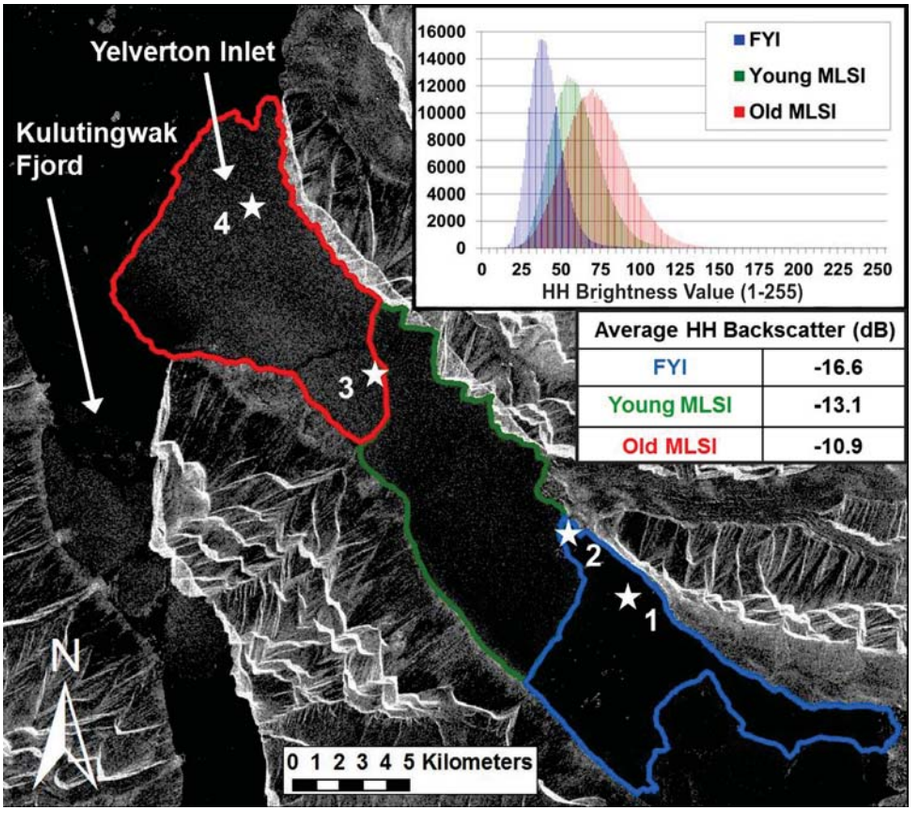

FIGURE 4. RADARSAT-2 image (wide beam mode, 5 March 2009, 20:17 UTC) showing ice type areas determined from ice thicknesses, ice core properties, GPR profiles, relative pixel brightness values (inset graph), and mean σ^0 values (inset table). Stars show ice core locations. RADARSAT-2 Data and Products © MacDonald, Dettwiler and Associates Ltd. All Rights Reserved.

(Jeffries and Sackinger, 1990b). These observations together suggest that the ice at the mouth of Yelverton Inlet in 2009 was MLSI.

The remaining two core sites (1 and 2) are located in the ice type found at the rear of Yelverton Inlet. The measured depths at Cores 1 and 2 corroborate GPR measurements indicating an average ice thickness of 1.66 m in this area (Fig. 1, Part c), the thinnest ice found in the study. This ice has a darker SAR signature (lower backscatter, mean $\sigma^0 = -16.6$ dB) than the other areas, with the exception of several bright spots, which were identified in the field as icebergs (Fig. 4). Salinities >1 psu within the first meter of ice thickness (see Cores 1, 2 in Fig. 2, Part a) limit the penetration of SAR signals, resulting in a signature largely dictated by surface scattering (Johnston and Timco, 2008; Shokr and Sinha, 1995). The local ice surface in this protected channel was observed in the field to be fairly smooth, with the exception of the frozen-in icebergs. The ice had very low variations in GPR-derived ice thicknesses (Fig. 1, Part c; standard deviation of 0.05 m) and no visible hummocks or ridging. The specular reflection of much of the SAR energy away from the sensor, as a function of this relatively smooth surface, explains the dark SAR signature (Johnston and Timco, 2008). These observations suggest that the ice at the rear of Yelverton Inlet is FYI.

The ice in central Yelverton Inlet features a darker signature (mean $\sigma^0 = -13.1$ dB) than the MLSI at the front of the inlet, but a lighter tone and more variable texture than the FYI at the rear (Fig. 4, Insets). The surface ridging characteristic of old MLSI was not observed over this area. Regional GPR-derived ice thickness measurements average 1.81 m with a standard deviation of 0.23 m, indicating greater variability than was measured in the FYI (Fig. 1, Part c). There are no ice core measurements from this ice area, which limits the confidence associated with assigning it an ice type. As the ice thicknesses and SAR brightness values place this region between the MLSI and the FYI, it is classified as Young MLSI. Dowdeswell and Jeffries (in press) describe a similar ice type occurring elsewhere in the Canadian High Arctic and Greenland: young MYI which remains stable due to the protection of a fiord but typically breaks up or melts out every few years.

GENERAL MLSI CHANGES IN YELVERTON BAY

The determination of sea ice types in 2009 allows for the identification of MLSI for other years with available imagery. The oblique air photos from 1950 show ice covering the ~30 km length of Yelverton Bay. Air photos from 1959 indicate the presence of 932.6 km^2 of MLSI, identifiable by its rolling surface and linear meltponds, in Yelverton Inlet and covering Yelverton Bay to approximately the same extent as in 1950 (Fig. 5, Part a). The identification of several matching ice features on all imagery between 1950 and 2005 confirmed that the main MLSI body in Yelverton Bay was stable over the entire period. The ice features that could be tracked over this period include a large ice island (3.82 km × 1.4 km) in the center of Yelverton Bay, an ice island (1.26 km × 0.38 km) 4.5 km west of the Petersen Ice Shelf, and a large crack running from Wootton Peninsula NE into the MLSI.

The only observed variations in the Yelverton Bay MLSI between 1959 and 2005 occurred along its outermost edge between the Milne Ice Shelf and Wootton Peninsula, where it was exposed to the shifting Arctic Ocean ice pack. An ERS-1 image from 19 May 1993 indicated changes in MLSI extent of ~10–100 m along this front since 1959. RADARSAT-1 images between 2000 and 2005 indicate that new MLSI extended ~3–5 km further into the Arctic Ocean than in 1993, with the still-intact old MLSI in Yelverton Bay behind it. This pattern of long-term stability dramatically changed in August 2005, as illustrated by RADARSAT-1 imagery (Fig. 5, Parts c–e). A 5 August image (Fig. 5, Part c) shows Yelverton Bay before any fracturing or breakup has occurred, with both the old and newer MLSI intact and bordered by Arctic Ocean pack ice. By August 8 (Fig. 5, Part d), ~330 km^2 of the newer MLSI from outer Yelverton Bay had broken away and is seen floating in open water. An 18 August image (Fig. 5, Part e) shows that 690 km^2 of the older MLSI had broken away in several large blocks from Yelverton Inlet, with the innermost break occurring at the location of a preexisting fracture (Fig. 5, Part d). Figure 5, Part e, also shows the formation of a new fracture deep in Yelverton Inlet. This MLSI loss occurred in tandem with a calving of 20% of the Petersen Ice Shelf and the rapid breakup of the Ayles Ice Shelf in August 2005 (Copland et al., 2007).

By September 2005, the large MLSI fragments had refrozen into the FYI matrix in Yelverton Bay, where they remained for the following three summers. A RADARSAT-1 image from 14 February 2008 confirms that the MLSI remnants were still frozen in Yelverton Bay; GPR measurements conducted on one of these pieces in April 2008 indicated ice thicknesses of up to 7 m (D. R. Mueller, unpublished data). MODIS images between 30 July and 31 August 2008 show the MLSI fragments breaking into smaller pieces and drifting out of Yelverton Bay, along with the MLSI at the mouth of Kulutingwak Fiord. A 16 August 2008 MODIS scene also shows open water at the rear of Yelverton Inlet; this supports the field-based determination that the ice present there the following year was FYI.

By the end of the 2008 melt season, only a small plug of MLSI was left intact at the mouth of Yelverton Inlet. The extent of this MLSI plug was quantified in the 2009 ASTER mosaic, and polygon differencing between the 1959 and 2009 mosaics indicate a total loss of 90% of the MLSI area in Yelverton Bay over the 50-year period (Fig. 5, Parts a and b). A MODIS image from 22 August 2010 indicates that the MLSI which had remained in Yelverton Inlet through summer 2009 has now broken away (Fig. 6). Yelverton Bay and Inlet therefore became free of MLSI by late summer 2010, a situation unprecedented in the historical record.

WOOTTON PENINSULA ICE SHELF CHANGES

The 2005 breakup event in Yelverton Bay was not limited to MLSI; 1950 and 1959 air photos and 1993–2005 SAR imagery (Table 1) also indicate the existence of a small, unnamed ice shelf in the protected cove to the east of Wootton Peninsula on the western edge of Yelverton Bay (Fig. 7). Identified as ice shelf ice (but unnamed) by Jeffries (1987), the 'Wootton Peninsula Ice Shelf' features a rolling surface texture, linear melt ponds (Fig. 7, Part a), and a bright return and ribbed texture in SAR imagery (Fig. 7, Part b). Polygon differencing between the 1959 air photo mosaic and the July 2009 ASTER image (Fig. 7, Part c) indicate a total loss of 16.44 km^2 of this ice shelf (65.6% of its area). This reduction occurred in two phases: the 18 August 2005 RADARSAT image shows ~8 km^2 of this ice shelf being removed during the Yelverton Bay MLSI reduction, and MODIS imagery shows the loss of the

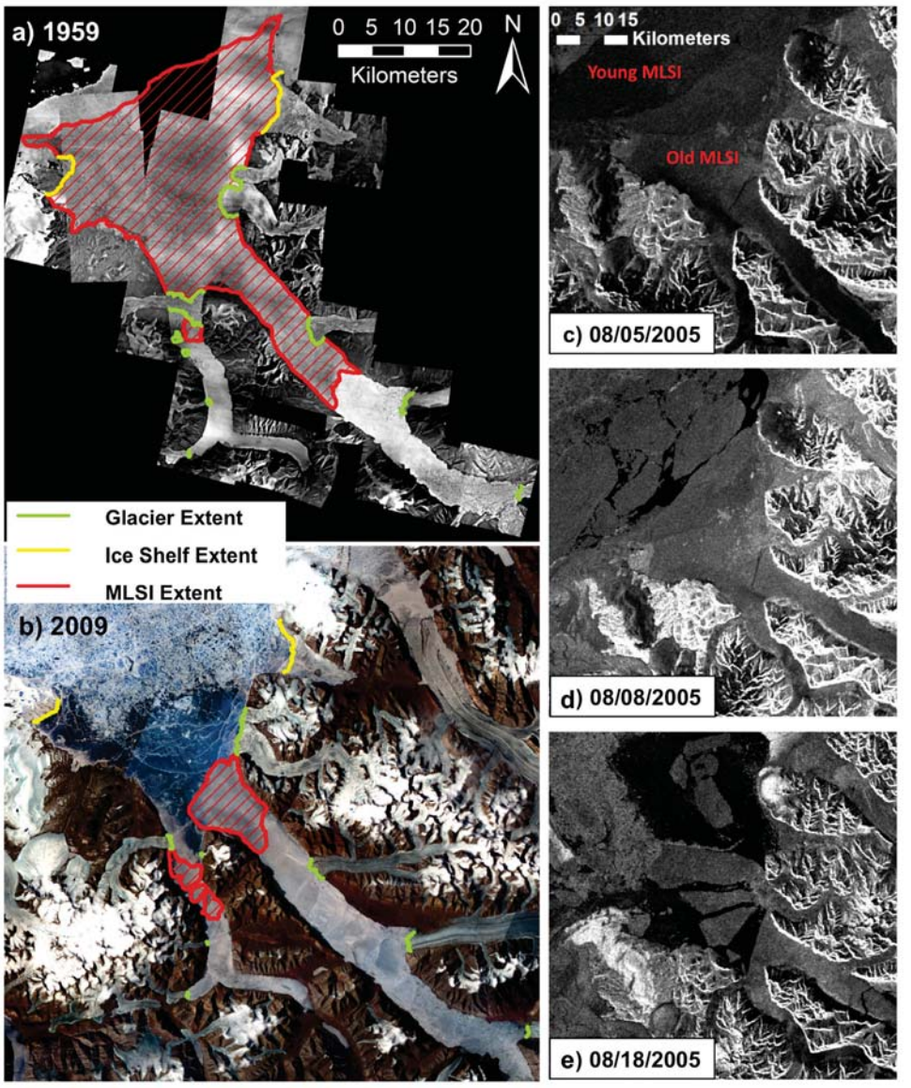

FIGURE 5. Changes in ice extent over 50 years in Yelverton Bay. (a) Air photo mosaic, June–August 1959. (b) ASTER mosaic, July 2009. (c–e) RADARSAT-1 ScanSAR Wide images showing the August 2005 MLSI breakup in Yelverton Bay. (c) 5 August 2005 20:15 UTC; old and new MLSI intact. (d) 8 August 2005 20:28 UTC; younger MLSI begins to break away. (e) 18 August 2005 20:36 UTC; old MLSI has broken at the mouth of the inlet and moved into outer Yelverton Bay.

remaining ice shelf ice between 6 and 16 August 2008 (cloud cover obscures exact timing). The maintenance of this ice shelf while being bordered by stable MLSI, and the subsequent loss following the 2005 MLSI removal, highlights the importance of MLSI buffering for the survival of ice shelves (Copland et al., 2007; Reeh et al., 2001). This buffering relationship has also been identified elsewhere; for example, Higgins (1989, 1991) noted that several North Greenland glaciers are maintained because they are confined by semi-permanent sea ice in the surrounding fjords. Observation of the MLSI at the edge of the Mertz Glacier tongue, East Antarctica, also suggests that it plays an important role in ice tongue/ice shelf stability (Massom et al., 2010).

KULUTINGWAK FIORD ICE TYPE CHANGES

Changes in glacier extents and reductions in MLSI in Yelverton Bay have led to significant changes in the ice types that are present in adjacent waterways. Besides those already described, another example of these changes occurred in northern Kulutingwak Fiord (Fig. 1). In the 1959 air photo mosaic (Fig. 5, Part a), a floating glacier terminus and associated icebergs can be seen blocking the mouth of Kulutingwak Fiord. However, by 2009 this glacier no longer extended into the fiord (Figs. 4; 5, Part b). Instead, several large blocks with a bright SAR signature covered this region, with a backscatter similar to that of the old MLSI identified at the mouth of Yelverton Inlet (Fig. 4). The ice surrounding these blocks had a dark SAR signature and smooth texture similar to that found at the southern end of Yelverton Inlet (Fig. 4), suggesting that they were FYI; this is confirmed by the presence of open water in this region the previous year. By 2010, a 3 March RADARSAT-2 scene indicates that much of this old MLSI had melted or drifted out of Kulutingwak Fiord, with only 2.3 km^2 of MLSI remaining in a matrix of FYI.

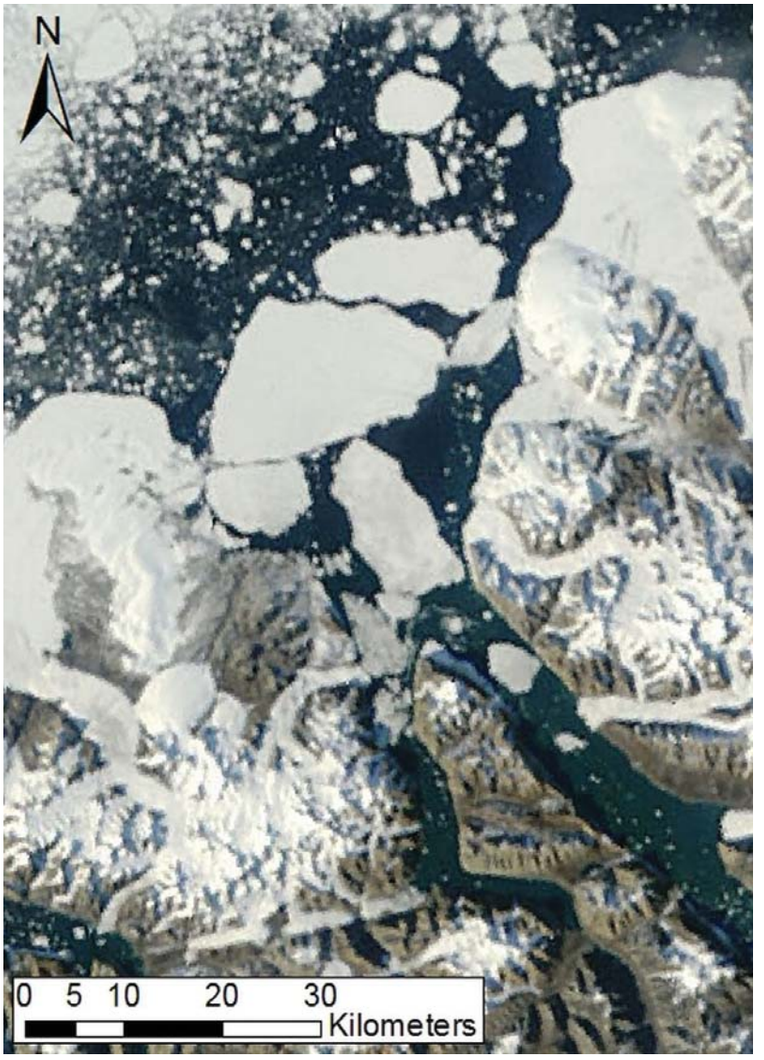

FIGURE 6. MODIS TERRA image (22 August 2010, 22:05 UTC) showing open water and floating ice in Yelverton Bay and Yelverton Inlet.

Summary

Large-scale reductions of ice shelf ice and MLSI in Yelverton Bay and Yelverton Inlet have occurred over the last 100 years, in tandem with glacial retreat and ice shelf losses along most of the northwest coast of Ellesmere Island. At the start of the 20th century an ice shelf covered Yelverton Bay, as it did along much of the NW Ellesmere Island coast. Between 1935 and 1946, the ice shelf ice in Yelverton Bay was replaced with MLSI, which survived for up to 70 years. The loss of MLSI from Yelverton Bay was dominated by the single loss of 690 km^2 of old MLSI in August 2005. This 2005 event was preceded by the loss of a border of ~330 km^2 of newer MLSI to the north of it, leaving open water at the

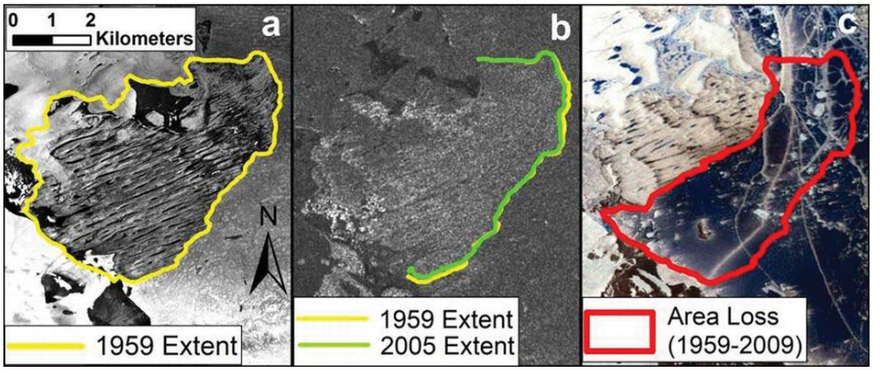

FIGURE 7. Changes to Wootton Peninsula Ice Shelf between 1959 and 2009. (a) Air photo from 13 August 1959. (b) RADARSAT-1 Standard Beam image (16 July 2005, 19:58 UTC) overlain with 1959 and 2005 ice shelf extents. (c) ASTER image (16 July 2009, 20:41 UTC) showing area loss of Wootton Peninsula Ice Shelf.

old MLSI front for several days. The 2005 breakup of the Yelverton MLSI occurred shortly before losses to the Petersen and Wootton Peninsula Ice Shelves, which had previously been buffered by persistent MLSI coverage across Yelverton Bay. Following the 2005 breakup event, sea ice in Yelverton Bay has consisted of displaced MLSI remnants, which were removed in 2008, and first year sea ice. The remaining Yelverton Inlet MLSI was measured in 2009 to be an average of 2.58 m thick, with a distinct layering of fresh ice over saline ice that was consistently identifiable as an internal reflector in GPR records. GPR was found to be an effective tool to determine MLSI thickness, with the qualification that adequate *in situ* thickness measurements are required for calibration of radar velocity.

The last remaining MLSI in the area broke away in August 2010 (Fig. 6), creating an MLSI-free Yelverton Bay and Inlet, unprecedented in recorded history. This loss is consistent with rising air temperatures in this region, with NCEP/NCAR reanalysis indicating a rise in mean annual temperature of 0.37 °C decade^{-1} for the nearby Ayles Ice Shelf between 1948 and 2006 (Copland et al., 2007), and Lesins et al. (2010) reporting a rise in mean annual temperature of ~3.2 °C from instrumental records at Eureka over the period 1972–2007. The loss of perennial sea ice here is also consistent with the overall decreases in sea ice extent and thickness occurring elsewhere in the Arctic. Higher proportions of younger, weaker sea ice along northern Ellesmere Island will limit the potential for regrowth of the MLSI which has historically buffered the margins of glaciers and ice shelves in this region.

Acknowledgments

We thank Colleen Mortimer for assistance in data collection, and the Polar Continental Shelf Program (PCSP) for assistance with field logistics. This is PCSP contribution #010-11. ASTER data courtesy of NASA; RADARSAT-1 and ERS data were provided by the Alaska Satellite Facility; RADARSAT-2 imagery was provided by the Canadian Ice Service, Environment Canada. Funding contributions came from Natural Sciences and Engineering Research Council of Canada, Canada Foundation for Innovation, Ontario Research Fund, and the University of Ottawa. The authors thank the Nunavut Research Institute and communities of Grise Fiord and Resolute Bay for permission to conduct this research.

References Cited

Alt, B., Wilson, K., and Carrieres, T., 2006: A case study of old-ice import and export through Peary and Sverdrup Channels in the Canadian Arctic Archipelago: 1998–2005. *Annals of Glaciology*, 44: 329–338.

Annan, A. P., 2002: GPR—History, trends, and future developments. *Subsurface Sensing Technologies and Applications*, 3(4): 53–270.

Askne, J., and Dierking, W., 2008: Sea ice monitoring in the Arctic and Baltic Sea Using SAR. *In* Barale, V., and Gade, M. (eds.), *Remote Sensing of the European Seas.* Dordrecht: Springer Science, 383–398.

Bradford, J. H., Dickins, D. F., and Brandvik, P. J., 2010: Assessing the potential to detect oil spills in and under snow using airborne ground-penetrating radar. *Geophysics*, 75(2): G1–G12.

Braun, C., Hardy, D. R., Bradley, R. S., and Sahanatien, V., 2004: Surface mass balance of the Ward Hunt Ice Rise and Ward Hunt Ice Shelf, Ellesmere Island, Nunavut, Canada. *Journal of Geophysical Research,* 109: D22110, http://dx.doi.org/10.1029/2004JD004560.

Copland, L., Mueller, D., and Weir, L., 2007: Rapid loss of the Ayles Ice Shelf, Ellesmere Island, Canada. *Geophysical Research Letters*, 34: L21501, http://dx.doi.org/10.1029/2007GL031809.

Crary, A. P., 1958: Arctic ice islands and ice shelf studies, part I. *Arctic*, 11(1): 3–42.

Crary, A. P., 1960: Arctic ice islands and ice shelf studies, part II. *Arctic*, 13(1): 32–50.

Dowdeswell, J., and Jeffries, M. O., in press: Arctic ice shelves: an introduction. *In* Copland, L., and Mueller, D. R. (eds.), *Arctic Ice Shelves and Ice Islands*. Dordrecht: Springer SBM.

England, J., Lakeman, T. R., Lemmen, D. S., Bednarski, J. M., Stewart, T. G., and Evans, D. J. A., 2008: A millennial-scale record of Arctic Ocean sea ice variability and the demise of the Ellesmere Island ice shelves. *Geophysical Research Letters,* 35: L19502, http://dx.doi.org/10.1029/2008GL034470.

Environment Canada, 2009: Weather Data: Canadian Climate Normals: Alert and Eureka <http://www.climate.weatheroffice.ec.gc.ca/climate_normals/index_e.html>.

Hattersley-Smith, G., 1955: Northern Ellesmere Island, 1953 and 1954. *Arctic,* 8(1): 3–36.

Hattersley-Smith, G., 1957a: The Ellesmere ice shelf and the ice islands. *Canadian Geographer*, 9: 65–70.

Hattersley-Smith, G., 1957b: The rolls of the Ellesmere Ice Shelf. *Arctic*, 10: 32–44.

Higgins, A.K. 1989. North Greenland ice islands. *Polar Record*, 25(154): 207–212.

Higgins, A.K. 1991. North Greenland glacier velocities and calf ice production. *Polarforschung*, 60(1): 1–23.

Howell, S. E. L., Duguay, C. R., and Markus, T., 2009: Sea ice conditions and melt season duration variability within the Canadian Arctic Archipelago: 1979–2008. *Geophysical Research Letters*, 36: L10502, http://dx.doi.org/10.1029/2009GL037681.

Jeffers, S., Agnew, T. A., Alt, B. T., De Abreu, R., and McCourt, S., 2001: Investigating the anomalous sea ice conditions in the Canadian High Arctic (Queen Elizabeth Islands) during the summer of 1998. *Annals of Glaciology*, 33: 507–512.

Jeffries, M. O., 1987: The growth, structure and disintegration of Arctic ice shelves. *Polar Record*, 23(147): 631–649.

Jeffries, M. O., 1992: Arctic ice shelves and ice islands: origin, growth and disintegration, physical characteristics, structural-stratigraphic variability and dynamics. *Reviews of Geophysics*, 30: 245–267.

Jeffries, M. O., and Sackinger, W. M., 1990a: Airborne SAR characteristics of arctic ice shelves and multiyear landfast sea ice, and the detection of massive ice calvings and ice islands. *Geoscience and Remote Sensing Symposium*, IGARSS'89, 12th Canadian Symposium on Remote Sensing, Vancouver, Canada, 2715–2718.

Jeffries, M. O., and Sackinger, W. M., 1990b: Ice island detection and characterization with airborne synthetic aperture radar. *Journal of Geophysical Research*, 95(C4): 5371–5377.

Johnston, M. E., and Timco, G. W., 2008: *Understanding and Identifying Old Ice in Summer*. Ottawa: Canadian Hydraulics Centre, National Research Council.

Koenig, L. S., Greenaway, K. R., Dunbar, M., and Hattersley-Smith, G., 1952: Arctic ice islands. *Arctic*, 5: 67–103.

Kovacs, A., and Morey, R., 1978: Radar anisotropy of sea ice due to preferred azimuthal orientation of the horizontal *c*-axis of ice crystals. *Journal of Geophysical Research*, 83(C12): 6037–6049.

Kwok, R., 2006: Exchange of sea ice between the Arctic Ocean and the Canadian Arctic Archipelago. *Geophysical Research Letters*, 33: L16501, http://10.1029/2006GL027094.

Kwok, R., and Rothrock, D. A., 2009: Decline in Arctic sea ice thickness from submarine and ICESat records: 1958–2008. *Geophysical Research Letters*, 36: L15501, http://dx.doi.org/10.1029/2009GL039035.

Lesins, G., Duck, T. J., and Drummond, J. R., 2010: Climate trends at Eureka in the Canadian High Arctic. *Atmosphere-Ocean,* 48: 59–80, http://dx.doi.org/10.3137/AO1103.2010.

Maslanik, J. A., Fowler, C., Stroeve, J., Drobot, S., Zwally, J., Yi, D., and Emery, W., 2007: A younger, thinner Arctic ice cover: increased

potential for rapid, extensive sea-ice loss. *Geophysical Research Letters*, 34: L24501, http://dx.doi.org/10.1029/2007GL032043.

Maslanik, J., Stroeve, J., Fowler, C., and Emery, W., 2011: Distribution and trends in Arctic sea ice age through spring. Geophysical Research Letters, 38: L13502, http://dx.doi.org/10.1029/2011GL047735.

Massom, R. A., Giles, A. B., Fricker, H. A., Warner, R. C., Legresy, B., Hyland, G., Young, N., and Fraser, A. D., 2010: Examining the interaction between multi-year landfast sea ice and the Mertz Glacier Tongue, East Antarctica: another factor in ice sheet stability? *Journal of Geophysical Research*, 115: C12027, http://dx.doi.org/10.1029/2009JC006083.

Melling, H., 2002: Sea ice of the northern Canadian Arctic Archipelago. *Journal of Geophysical Research,* 107(C11): 3181, http://dx.doi.org/10.1029/2001JC001102.

Mortimer, C. A., 2011: *Quantification of Changes for the Milne Ice Shelf, Nunavut, Canada, 1950–2009*. MSc thesis, Department of Geography, University of Ottawa.

Mueller, D. R., Vincent, W. F., and Jeffries, M. O., 2006: Environmental gradients, fragmented habitats, and microbiota of northern ice shelf cryoecosystem, Ellesmere Island, Canada. *Arctic, Antarctic, and Alpine Research*, 38(4): 593–607.

Mueller, D. R., Copland, L., Hamilton, A., and Stern, D., 2008: Examining Arctic ice shelves prior to the 2008 breakup. *EOS, Transactions of the American Geophysical Union*, 89(49): 502–503.

Nghiem, S. V., Chao, Y., Neumann, G., Li, P., Perovich, D. K., Street, T., and Clemente-Colón, P., 2006: Depletion of perennial sea ice in the East Arctic Ocean. *Geophysical Research Letters*, 33: L17501, http://dx.doi.org/10.1029/2006GL027198.

Nghiem, S. V., Rigor, I. G., Perovich, D. K., Clemente-Colón, P., Weatherly, J. W., and Neumann, G., 2007: Rapid reduction of Arctic perennial sea ice. *Geophysical Research Letters,* 34: L19504, http://dx.doi.org/10.1029/2007GL031138.

NSIDC [National Snow and Ice Data Center], 2011: Summer 2011: Arctic sea ice near record lows. *Arctic Sea Ice News and Analysis*: 4 October 2011, http://nsidc.org/arcticseaicenews/2011/100411.html.

Nyland, D., 2004: Profiles of floating ice in arctic regions using GPR. *The Leading Edge,* 23: 665–668.

Polunin, N., 1955: Attempted dendrochronological dating of ice island T-3. *Science*, 122(3181): 1184–1186.

Reeh, N., Thomsen, H. H., Higgins, A. K., and Weidick, A., 2001: Sea ice and the stability of North and Northeast Greenland floating glaciers. *Annals of Glaciology,* 33: 474–480.

Rigor, I. G., and Wallace, J. M., 2004: Variations in the age of Arctic sea-ice and summer sea-ice extent. *Geophysical Research Letters*, 31: L09401, http://dx.doi.org/10.1029/2004GL019492.

Rothrock, D. A., Yu, Y., and Maykut, G. A., 1999: Thinning of the Arctic sea-ice cover. *Geophysical Research Letters*, 26(23): 3469–3472.

Serreze, M. C., Holland, M. M., and Stroeve, J., 2007: Perspectives on the Arctic's shrinking sea-ice cover. *Science*, 315(5818): 1533–1536.

Shokr, M., and Sinha, N. K., 1995: Physical, electrical and structural properties of Arctic sea ice observed during SIMMS'92 experiment. Environment Canada, Atmospheric Environment Service, Research Report No. 95-005: p. 148.

Stroeve, J., Holland, M. M., Meier, W., Scambos, T., and Serreze, M., 2007: Arctic sea ice decline: faster than forecast. *Geophysical Research Letters*, 34: L09501, http://dx.doi.org/10.1029/2007GL029703.

Stroeve, J. C., Serreze, M. C., Holland, M. M., Kay, J. E., Maslanik, W. N., Meier, W. N., and Barrett, A. P., 2011: The Arctic's rapidly shrinking sea ice cover: A research synthesis. *Climatic Change*, 110(3–4): 1005–1027, http://dx.doi.org/10.1007/s10584-011-0101-1.

Tivy, A., Howell, S. E. L., Alt, B., McCourt, S., Chagnon, R., Crocker, G., Carrieres, T., and Yackel, J. J., 2011: Trends and variability in summer sea ice cover in the Canadian Arctic based on the Canadian Ice Service Digital Archive, 1960–2008 and 1968–2008. *Journal of Geophysical Research*, 116: C03007, http://dx.doi.org/10.1029/2009JC005855.

Vincent, W. F., Gibson, J. A. E., and Jeffries, M. O., 2001: Ice shelf collapse, climate change and habitat loss in the Canadian High Arctic. *Polar Record*, 37: 133–142.

Wadhams, P., 2000: *Ice in the Ocean*. Amsterdam: Gordon and Breach Science Publishers.

Woodward, J., and Burke, M. J., 2007: Applications of ground-penetrating radar to glacial and frozen materials. *Journal of Environmental & Engineering Geophysics*, 12(1): 69–85.

MS accepted December 2011